New dynamic three-dimensional MRI technique for shoulder kinematic analysis

Jérôme Pierrart, Marie-Martine Lefèvre-Colau, Wafa Skalli, Valérie Vuillemin, Emmanuel H. Masmejean, Charles A. Cuénod, Thomas M. Gregory

Technical Note

New Dynamic Three-Dimensional MRI Technique for Shoulder Kinematic Analysis

Jérôme Pierrart, MD,[1,2] Marie-Martine Lefèvre-Colau, MD, PhD,[3] Wafa Skalli, PhD,[1] Valérie Vuillemin, MD,[4] Emmanuel H. Masmejean, MD, PhD,[2] Charles A. Cuénod, MD, PhD,[3] and Thomas M. Gregory, MD, PhD[2]*

Purpose: To establish a new imaging technique using dynamic MRI three-dimensional (3D) volumetric acquisition in real-time, on six normal shoulders for the analysis of the 3D shoulder kinematics during continuous motion.

Materials and Methods: At first, a standard static acquisition was performed. Then, fast images were obtained with a multi-slice 3D balanced gradient echo sequence to get a real time series during the initial phase of shoulder abduction. Subsequently, the images were reconstructed; registered and the translational patterns of the humeral head relative to the glenoid and the size of the subacromial space were calculated. Additionally, the intraobserver reproducibility was tested.

Results: The maximal abduction was on average 43° (30° to 60°) and the mean width of the subacromial space was 7.7 mm (SD: ± 1.2 mm). Difference between extreme values and average values was low, respectively 2.5 mm on X-axis, 2 mm on Y-axis, 1.4 mm for the width of the subacromial space and 1.2° for the measure of the glenohumeral abduction.

Conclusion: This study reported a dynamic MRI protocol for the monitoring of shoulder 3D kinematics during continuous movement. The results suggest that there is no superior shift of the humeral head during the first phase of abduction.

Key Words: shoulder kinematic; real time MRI; 3D kinematic

MUSCULOSKELETAL DISEASES OF the shoulder are frequent, involving up to 30% of the population when considering the rotator cuff diseases (RCD) alone (1). Shoulder motion is the result of the synergic and combined movement of both the scapulohumeral and the scapulothoracic joints. RCD are associated with alteration of the shoulder girdle motion (2). However, to date, except ultrasound, only static imaging techniques are available (MRI, computed tomography scan) for the detection of RCD. Hence, the causes of RCD are misunderstood, leading very often to nonoptimal medical or surgical management. To address the above-mentioned issues, there is the need for noninvasive imaging techniques assessing the shoulder complex kinematic during arm elevation.

So far, shoulder kinematic has been analyzed in cadaver studies that provide very little information on the complex muscle activation pattern of the shoulder during the active arm elevation (3). Reliability of methods based on external markers is controversial because of the known shift between the skin and the bone structures during shoulder motion (4,5). Conventional X-rays (6–8) and the EOSTM Low Dose Stereography System (9) have been used for the analysis of the humeral head translation relative to the glenoid, but in these studies, the analysis of the shoulder girdle motion is only pseudo-kinematic. Bey et al (10) and Zhu et al (11) have validated a biplanar fluoroscopic technique assessing in 3D the bone structures shoulder kinematic. The limits of such a technique is the patient radiation exposure and the lack of possibility to get a future direct analysis of the soft tissues, i.e., the rotator cuff. In vivo MRI, two-dimensional (2D) or three-dimensional techniques (2,12–19) have been established for pseudo-kinematic analysis of the shoulder (in several static positions), but here again, these techniques do not provide data on the "real" shoulder kinematics, i.e., during continuous movement of the arm. A 2D MRI Shoulder kinematic analysis during continuous movement of the arm has been assessed (20,21), but the quality of the measures relies on the image acquisition frame steadiness in one plane, which is highly challenging and not feasible in routine clinical setting.

[1]Laboratory of Biomechanics, Arts et métiers ParisTech, France.
[2]Orthopaedic Surgery and traumatology, European Hospital Georges Pompidou, APHP, Université Paris Descartes, Sorbonne Paris Cité, Faculté de Médecine, Paris, France.
[3]Physical Medicine and Rehabilitation Unit, Cochin Hospital, APHP, Université Paris Descartes, Sorbonne Paris Cité, Faculté de Médecine, Paris, France.
[4]Radiology Unit, European Hospital Georges Pompidou, APHP, Université Paris Descartes, Sorbonne Paris Cité, Faculté de Médecine, Paris, France.
*
France. E-mail: thomas.gregory@egp.aphp.fr
DOI 10.1002/jmri.24204
View this article online at wileyonlinelibrary.com.

Multi-slice cine-MRI that provides 3D volumetric acquisition in real-time has been established for the detection of cardiovascular diseases and is nowadays used in routine clinical setting (22). In the field of musculoskeletal disorders, authors have attempted to use cine-MRI for knee kinematic evaluation (23,24). However, as far as we know, it has never been used for the detection of shoulder kinematics disorders.

The main goal of the present pilot study is to establish a new imaging technique using MRI 3D volumetric acquisition in real-time allowing shoulder kinematics analysis. The proof of concept is evaluated in six shoulders of four healthy volunteers. A second goal is to provide 3D continuous data of the translational patterns of the humeral head relative to the glenoid and of the changes in the subacromial space dimensions in the initial phase of the arm abduction.

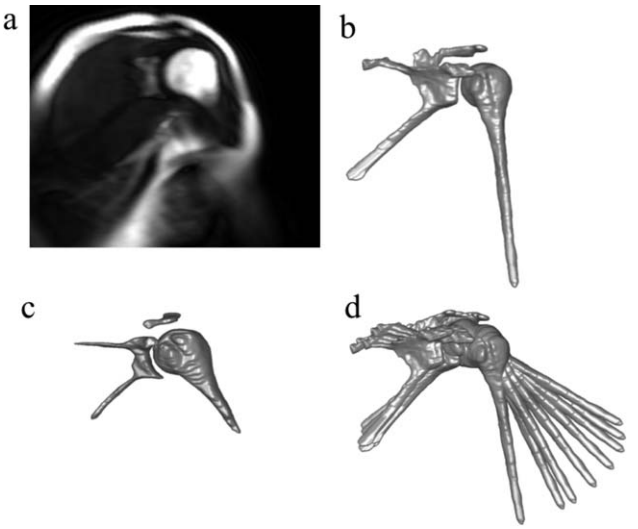

Figure 1. **a**: Image from the FIESTA dynamic acquisition (1 image among one of the seven datasets of 56 images). **b:** A 3D reconstruction at initial position from 3D T1-weighted gradient echo sequence. **c:** One intermediate position before registration from multi-slice 3D balanced echo gradient (FIESTA). **d:** Reconstruction at initial position and all intermediate positions after registration.

MATERIALS AND METHODS

A prospective study involving six shoulders of four healthy volunteers was carried out. A shoulder three-dimensional real-time MRI protocol was established and both the translational patterns of the humeral head relative to the glenoid and the changes in the subacromial space width were measured during arm abduction. The patient population consisted of six shoulders (four rights and two left) from four healthy volunteers (one male and three females, mean age: 34.2 years (30–45), mean height: 165 cm (range, 160–175 cm), mean weight: 54.2 kg (range, 45–60 kg). Before imaging, an expert shoulder surgeon verified the volunteers' normal shoulder physical examination and the lack of past history of any shoulder diseases or trauma. Each volunteer was given an informed consent form to read and sign and the local ethics committee approved all parts of this study.

Shoulder 3D Real-Time MRI Protocol

A standard protocol of image acquisition, data processing and analysis was established. It includes three steps that are described in details below: acquisition of 3D dataset of MR images; 3D reconstructions and registration; measures of the translational patterns of the humeral head relative to the glenoid and of the width of the subacromial space.

First Step: Acquisition of Dynamic Volume Dataset of MR Images

Each volunteer was placed in supine position inside the closed-bore MR scanner (Sigma 1.5 Tesla [T] system, General Electric-Milwaukee, WI) fitted with a dedicated phased-array shoulder coil. The patient was slightly shifted toward the side opposite to the arm of interest to get more room for the arm abduction and to place the shoulder nearest to the magnet center. In this initial position, the arm was lying along the body, elbow flexed by 90° and the hand resting on the chest wall. This position defined the reference position of our study. Before starting the dynamic acquisition process, each volunteer was given precise details of the procedure and instructions on how they should move their arm: on command, the arm had to abduct slowly in the scapula blade direction (see description of dynamic acquisition, below, for information about speed of movement).

The scapulohumeral joint was totally captured within the MR field of scanning. In each case, oblique coronal images on the frame of the scapula were implemented. Before starting the dynamic acquisition process, a standard static acquisition was performed with a view to obtaining high-resolution reference images. A coronal 3D T1 weighted gradient echo sequence was used, with a flip angle of 20°, a repetition time (TR) of 6.2 ms, an echo time (TE) of 2.7 ms, a field of view (FOV) 35 × 35 with a 160 × 160 acquisition matrix, a 512 zero filling interpolation, and 2 mm thick continuous sections. Total data acquisition time was 1 min 30 s.

Then, the volumetric dynamic acquisition process was performed. It aimed to get a real time series during the shoulder motion. Fast images were obtained with a multi-slice 3D balanced gradient echo sequence (FIESTA: Fast Imaging Employing Steady sTate Acquisition) with a flip angle of 65°, a TR of 3.6 ms, a TE of 1.3 ms, a 35 × 35 FOV with a 220 × 220 acquisition matrix with a 512 zero filling interpolation, a bandwidth (BW) of 50 kHz, 14 sections of 10 mm thickness leading, with a fourth factor of zero filling interpolation in the z direction, to a total of 56 overlapped sections (Fig. 1a). The acquisition phase lasted four seconds and was repeated seven times (phases) for a total acquisition time of 28 s, during which the volunteer was performing a slow and continuous abduction until his/her elbow abuts against the inner wall of the scanner bore (i.e., the volunteer performed one abduction motion in 28 s). Each of seven phases gave one complete series of 56

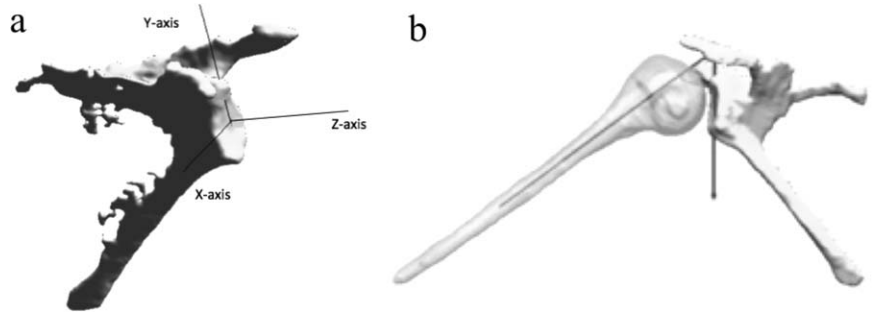

Figure 2. a: The figure represents a scapula bone with its coordinate system. The anteroposterior axis (X-Axis) was directed to coracoid, Y-axis as craniocaudal axis, and Z-axis as vector product of Y and X axes. **b:** Glenohumeral abduction level was defined by intersection of both humeral shaft axis and the plane on the glenoid.

overlapped sections at a different position of the shoulder from the resting reference position to the maximal abduction possible within the magnet. Careful positioning of field of view and obliquity of the coronal plane was necessary to ensure that the superior: part of the humeral bone and entire scapula were both fully captured during the entire series.

Total examination time was 10 to 15 min per shoulder, including timeout and installation of the patient. After the scanning was completed and radiologists had confirmed the absence of shoulder's diseases, MRI images were anonymized and transferred on compact disc (CD) for further analysis.

Second Step: 3D Reconstruction and Registration (Fig. 1)

Data processing and analysis was performed on a standard PC. Commercial software (AVIZO®, Visualization Science Group, VSG; Burlington, MA) was used for shoulder modeling. The software allows a semi-automatic segmentation for 3D reconstruction of each series. After a preliminary automatic computer-based segmentation of the trabecular bone, the cortical bone was manually enhanced on each slice. A precise 3D reconstruction was gained from the standard static acquisition, using the coronal T1 sequence at rest, based on a set of 340 slices. This 3D model was used as a reference model for the registration phase. In parallel, seven coarser reconstructions, corresponding to seven different abducting positions and so-called "intermediary models," were obtained from the coronal FIESTA 3D dynamic sequence based on the set of 56 slices obtained per phase. From Avizo package, an unconstrained filter smoothed the reconstructions without volume alteration. Then, Geomagic® software package (Geomagic, Morrisville, NC) was used to realize semi-automatic registration by best-fit alignment of the reference model on intermediate models, with respect of their specific coordinates. The quality of the registration and the consistence between models were calculated by 3D analysis comparisons, based on selected areas of interest (namely glenoid surface, acromion inferior aspect, humeral head, and humeral shaft). Errors lower than 1 mm between areas of interest were tolerated. Consequently, this step results in a precise 3D model of the scapula and humerus in all positions of arm abduction.

Third Step: Measures of the Translational Patterns of the Humeral Head Relative to the Glenoid and of the Width of the Subacromial Space

The identification of different anatomical areas (humeral head, shaft and greater tuberosity of the humerus, acromion process, and glenoid of the scapula) was performed from the 3D model using specific software developed in the Laboratory of Biomechanics (Fig. 2). MatLab (MathWorks®, software) was used to compute, animate, and analyze the kinematics of the glenohumeral joint as follows.

A mean least squares ellipse was fitted on the contour of the glenoid region and subsequently the glenoid coordinate system was characterized: minor axis as anteroposterior axis (X), major axis as craniocaudal axis (Y), and Z-axis as vector product of X- and Y-axis (Fig. 2a). The center of the ellipse was used as the center of the glenoid coordinate system and X- and Y-axis defined the glenoid plane. For determining the central point of the humeral head, a sphere was fitted to the humeral surface of the humeral head. This central point was projected perpendicularly onto the glenoid plane and its location was defined in the glenoid coordinate system (17,25). Glenohumeral abduction is defined as the angle formed by the longitudinal axis of the humerus and the glenoid plane in abduction (15,16,26) (Fig. 2b). The width of the subacromial space was defined as the shortest distance between the superior aspect of the proximal humerus contour (humeral head or trochiter) and the inferior aspect of the acromion. Finally, two parameters were calculated for each shoulder position: the width of subacromial space and the modification of the center of the humeral head during arm motion in the glenoid coordinate system. At the maximal abduction level, the elbow abutted against the scanner inner wall. Consequently, this last position was considered as not physiological and subsequently not taken into consideration. The number of positions before abutment varied from one shoulder to the next according to patient-specific factors such as weight and size.

The intraobserver reproducibility was tested for one intermediate position of one shoulder. The 3D reconstruction of the same intermediate position was repeated 6 times, each reconstruction being followed by the registration step. The average value was considered as the reference value and the difference between the extreme value and the average value was

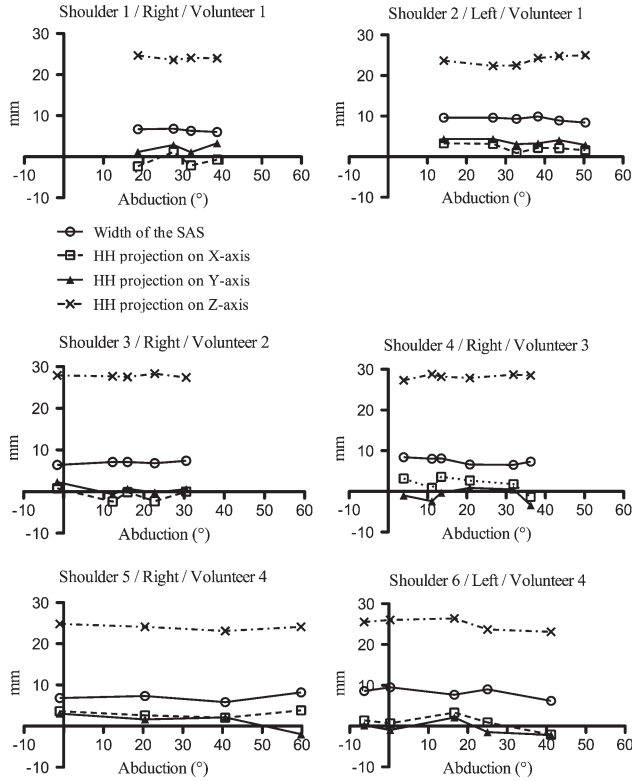

Figure 3. Width of the subacromial space (SAS) and location of humeral head center (HH) projection in glenoid coordinate system (X, Y, and Z), for all shoulders, during abduction before abutment.

calculated for three parameters: coordinates on the X- and Y-axes, width of the subacromial space and measure of the glenohumeral abduction.

RESULTS

The feasibility of acquiring dynamic MRI 3D images during continuous shoulder motion, of performing images reconstruction and registration leading to shoulder bone kinematics analysis, was validated for the six involved shoulders. The maximal glenohumeral abduction before abutment was on average 43° (from 30° to 60°).

Results for all shoulders are reported Figure 3. Over the analyzed range of motion, the width of the subacromial space was on average of 7.7 mm (SD: ±1.2). The distance between the humeral head center and the glenoid plane (Z-axis) was on average of 25.6 mm (SD: ± 2.1). The distance between the humeral head center projection and the glenoid center on the glenoid coordinate system was on average of 1 mm (SD: ±2.2) in the superior direction (Y-axis) and on average 1.1 mm (SD: ± 2) in the anterior direction (X-axis). The humeral head center projection was centered on the glenoid, the maximum observed deviation in the glenoid coordinate system (X or Y) being 4.4 mm.

Results for each of the six shoulders are reported Table 1. Over the analyzed range of abduction, both the width of the subacromial space and the center of the humeral head projection relative to the glenoid center were found to have low variability. For the width of the subacromial space, mean values over abduction were in the range 6.4 and 9.3 mm for the six shoulders, and the variations over abduction were in the range 0.8 to 3.3 mm. Figure 4 represents successive locations of the humeral head center projection regard to the glenoid for the each of the six shoulders during abduction.

Results of the intraobserver reproducibility test are reported in Table 2. Difference between extreme values and average values was 2.5 mm on X-axis, 2 mm on Y-axis, 1.4 mm for the width of the subacromial space, and 1.2° for the measure of the glenohumeral abduction.

DISCUSSION

A better knowledge of the normal and pathological shoulder kinematic will improve shoulder diseases diagnosis and treatment. However, to date, there is no existing imaging technique enabling the analysis of the 3D shoulder kinematics during continuous motion. Shoulder dynamic imaging used, to date, namely conventional radiographs and EOS™ in pseudo-kinematic, multi-postural MRI, cine MRI, and skin markers, provide questionable information about the real shoulder kinematics and need, at least, to be validated (4,5,9,12,14,16,20,21). MRI for the analysis of shoulder diseases has well-known advantages: it is noninvasive and provides high soft tissue contrast without ionizing radiations. However, the problem of acquiring volumetric image during continuous motion has to be solved (27). As far as we know, the dynamic MRI Protocol presented in this study allows, for the first time in the literature, the visualization of the shoulder bone kinematics in 3D during continuous movement of the arm. The feasibility of the protocol was validated on six shoulders.

Table 1
Mean Values of Measures During Abduction for Each of the Six Shoulders*

	SAS (mm)	X-axis (mm)	Y-axis (mm)	Z-axis (mm)
Shoulder 1	6.4 (6; 6.8)	−1 (−2.3; 1.2)	2.1 (1.1; 3.3)	24.1 (23.6; 24.7)
Shoulder 2	9.3 (8.4; 9.9)	2.2 (0.9; 3.3)	3.7 (2.9; 4.4)	23.8 (22.4; 25)
Shoulder 3	7 (6.4; 7.4)	−0.8 (−2.4; 0.8)	0.6 (−0.6; 2.3)	27.8 (27.4; 28.3)
Shoulder 4	7.5 (6.5; 8.4)	1.8 (−1.3; 3.6)	−1 (−3.4; 0.9)	28.2 (27.3; 28.8)
Shoulder 5	7 (5.8; 8.2)	3 (2; 3.8)	1.2 (−2; 3)	24 (23.1; 24.8)
Shoulder 6	8.2 (6.2; 9.5)	0.8 (−2.1; 3.3)	−0.5 (−2.2; 2.1)	25 (23.1; 26.4)

*X-axis, Y- axis, and Z- axis correspond to the coordinate of the projection of humeral head center on glenoid coordinate system; X-axis as anteroposterior axis, Y-axis as craniocaudal axis and Z- axis as normal to the glenoid plane. SAS = width of subacromial space.

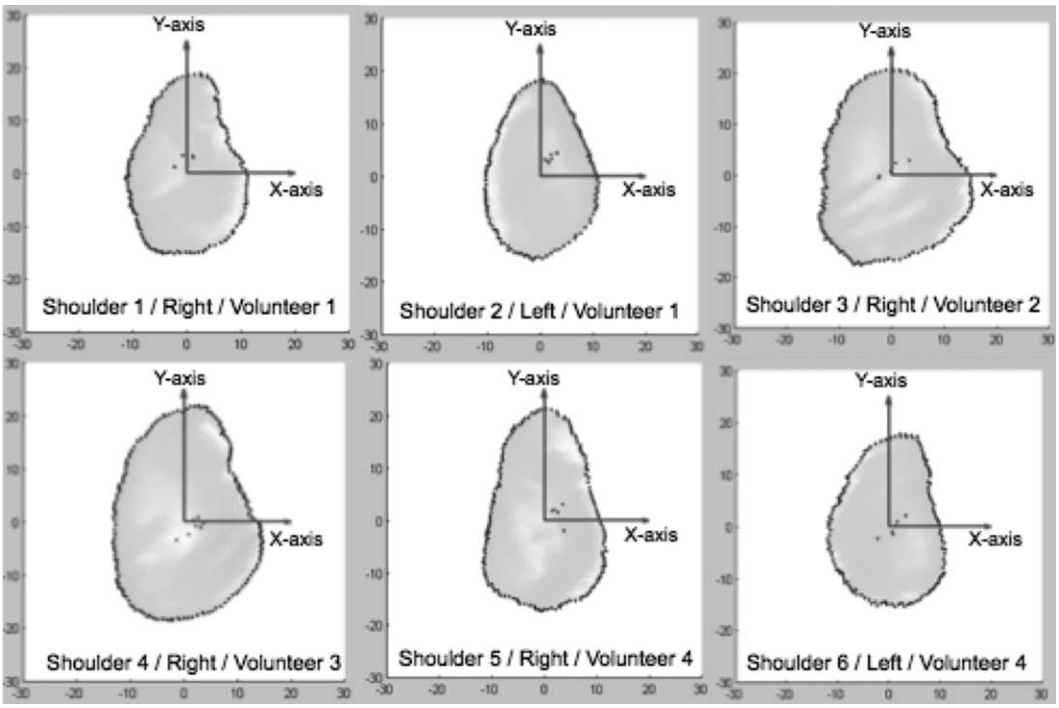

Figure 4. Representation of successive locations of humeral head center projection with regard to the glenoid. Each dot corresponds to one humeral head center projection. X-axis represents the anteroposterior direction and Y-axis represents the inferosuperior direction.

In a multi-positional MRI study, Graichen et al (12) reported that the dimension of the subacromial space was on average 7.0 mm (±1,6) at 30° of arm abduction. In our study, the dimension of the subacromial space was on average 7.7 mm (± 1.2), and was consistent during the first phase of the arm abduction (on average 43°, ranging from 30° to 60° in our series). From 10 "normal" shoulders imaged by 2D cine MRI, Beaulieu et al (20) reported that the distance of the projection of the humeral head center from the center of the glenoid was less than 3 mm over the entire motion, compared with 4.4 mm in our study, over the first 43° of arm abduction. Compared with our 3D MRI technique, the image acquisition frame stability interfered with the accuracy of the measure in 2D MRI techniques. These results suggest that there is no superior shift of the humeral head during the first phase of the shoulder abduction.

We are aware that this protocol is perfectible in many ways: In this study, a close bore scanner was used because of its better availability. This choice led to a restriction in the shoulder abduction (by on average 43°). However, the protocol described in this study could be easily transferred in an open-bore MRI scanner that would provide, in upright position, the bone structure kinematics up to the maximum range of abduction. In addition, only bone structures were assessed, which limits the ability of detecting RCD. Visualization of tendons and muscles, although not impossible, requires additional researches and will be worked out in further studies.

This study did not assess the interobserver reproducibility of the technique. Only the intraobserver reproducibility was evaluated. Considering all criteria (data on X-axis and Y-axis of the humeral head projection and width of the subacromial space), the difference between the extreme values and the average values were less than 2.5 mm, i.e., showing a good consistency. The interobserver reproducibility was not investigated because the segmentation of the images, in step two of the protocol, is very time-consuming. Consequently, although this study is the first successful attempt to analyze the shoulder kinematics by 3D MRI during continuous movement of the arm, this protocol need to be enhanced with a improvement of the computer-based segmentation of the images before being used in routine practice. Finally, each

Table 2
Intraobserver Reproductibility

N°	GH abd (°)	SAS (mm)	X-axis (mm)	Y-axis (mm)	Z-axis (mm)
1	32.8	9.3	0.9	3.1	22.5
2	34.8	9	−2.0	1.4	23.6
3	34.9	8	−2.7	2.2	22.4
4	34.8	9.4	−2.3	0.2	21.9
5	33.4	10.5	−1.7	−0.2	23
6	33.4	10.4	−2.0	−0.3	23.7
Average	34	9.4	−1.6	1.1	22.9
E.V.	(32.8; 34.9)	(8; 10.5)	(−2.7; 0.9)	(−0.3; 3.1)	(21.9; 23.7)

X-axis, Y- axis, and Z-axis correspond to the coordinate of the projection of humeral head center on glenoid coordinate system; X-axis as anteroposterior axis, Y-axis as craniocaudal axis, and Z-axis as normal to the glenoid plane; SAS = width of subacromial space; E.V. = extreme values; GH abd = level of glenohumeral abduction.

acquisition phase lasted for 4 s and was repeated 7 times. Consequently, the total acquisition time used in this dynamic was 28 s. This does not correspond to the "normal motion speed" of the shoulder, although; the definition of this "normal motion speed" is debatable. As the image noise is inversely proportional to the acquisition speed, the chosen speed balanced minimal images noise for getting good quality reconstructions against verging on the physiological speed of the shoulder motion. Consequently, compared with pseudo-kinematics imaging techniques, this protocol provides an important step forward toward the use of dynamic MRI for the detection of shoulder diseases, specially RCD, in routine practice (12,13,15,16).

In conclusion, this study reported a dynamic MRI protocol for the monitoring of the shoulder 3D bone kinematics during continuous movement of the arm. This is only a pilot study and the protocol need to be enhanced before being used in routine practice for the detection of rotator cuff diseases. However, the feasibility of this new imaging technique was shown on six normal shoulders. The results suggest that there is no superior shift of the humeral head during the first phase of the shoulder abduction.

ACKNOWLEDGMENTS

We thank L. Vancura and B. Lambert for their valuable assistance.

REFERENCES

1. Bodin J, Ha C, Chastang J-F, et al. Comparison of risk factors for shoulder pain and rotator cuff syndrome in the working population. Am J Ind Med 2012;55:605–615.
2. Graichen H, Stammberger T, Bonél H, et al. Three-dimensional analysis of shoulder girdle and supraspinatus motion patterns in patients with impingement syndrome. J Orthop Res 2001;19:1192–1198.
3. Billuart F, Devun L, Gagey O, et al. 3D kinematics of the glenohumeral joint during abduction motion: an ex vivo study. Surg Radiol Anat 2007;29:291–295.
4. Benoit DL, Ramsey DK, Lamontagne M, et al. Effect of skin movement artifact on knee kinematics during gait and cutting motions measured in vivo. Gait Posture 2006;24:152–164.
5. Hill AM, Bull AMJ, Dallalana RJ, et al. Glenohumeral motion: review of measurement techniques. Knee Surg Sports Traumatol Arthrosc 2007;15:1137–1143.
6. Paletta GA Jr, Warner JJ, Warren RF, et al. Shoulder kinematics with two-plane x-ray evaluation in patients with anterior instability or rotator cuff tearing. J Shoulder Elbow Surg 1997;6:516–527.
7. Yamaguchi K, Sher JS, Andersen WK, et al. Glenohumeral motion in patients with rotator cuff tears: a comparison of asymptomatic and symptomatic shoulders. J Shoulder Elbow Surg 2000;9:6–11.
8. Deutsch A, Altchek DW, Schwartz E, et al. Radiologic measurement of superior displacement of the humeral head in the impingement syndrome. J Shoulder Elbow Surg 1996;5:186–193.
9. Lagace P-Y, Billuart F, Ohl X, et al. Analysis of humeral head displacements from sequences of biplanar X-rays: repeatability study and preliminary results in healthy subjects. Comput Methods Biomech Biomed Engin 2012;15:221–229.
10. Bey MJ, Zauel R, Brock SK, et al. Validation of a new model-based tracking technique for measuring three-dimensional, in vivo glenohumeral joint kinematics. J Biomech Eng 2006; 128:604–609.
11. Zhu Z, Massimini DF, Wang G, et al. The accuracy and repeatability of an automatic 2D–3D fluoroscopic image-model registration technique for determining shoulder joint kinematics. Med Eng Phys 2012;34:1303–1309.
12. Graichen H, Bonel H, Stammberger T, et al. Subacromial space width changes during abduction and rotation–a 3-D MR imaging study. Surg Radiol Anat 1999;21:59–64.
13. Graichen H, Bonel H, Stammberger T, et al. Three-dimensional analysis of the width of the subacromial space in healthy subjects and patients with impingement syndrome. AJR Am J Roentgenol 1999;172:1081–1086.
14. Graichen H, Bonel H, Stammberger T, et al. A technique for determining the spatial relationship between the rotator cuff and the subacromial space in arm abduction using MRI and 3D image processing. Magn Reson Med 1998;40:640–643.
15. Graichen H, Hinterwimmer S, Von Eisenhart-Rothe R, et al. Effect of abducting and adducting muscle activity on glenohumeral translation, scapular kinematics and subacromial space width in vivo. J Biomech 2005;38:755–760.
16. Graichen H, Stammberger T, Bonel H, et al. Magnetic resonance-based motion analysis of the shoulder during elevation. Clin Orthop Relat Res 2000;154–163.
17. Graichen H, Stammberger T, Bonel H, et al. Glenohumeral translation during active and passive elevation of the shoulder - a 3D open-MRI study. J Biomech 2000;33:609–613.
18. Sans N, Richardi G, Fourcade D, et al. Cine-MRI of the shoulder. Normal aspects. J Radiol 1996;77:117–123.
19. Sahara W, Sugamoto K, Murai M, et al. The three-dimensional motions of glenohumeral joint under semi-loaded condition during arm abduction using vertically open MRI. Clin Biomech (Bristol, Avon) 2007;22:304–312.
20. Beaulieu CF, Hodge DK, Bergman AG, et al. Glenohumeral relationships during physiologic shoulder motion and stress testing: initial experience with open MR imaging and active imaging-plane registration. Radiology 1999;212:699–705.
21. Hodge DK, Beaulieu CF, Thabit GH III, et al. Dynamic MR imaging and stress testing in glenohumeral instability: comparison with normal shoulders and clinical/surgical findings. J Magn Reson Imaging 2001;13:748–756.
22. Bornstedt A, Nagel E, Schalla S, et al. Multi-slice dynamic imaging: complete functional cardiac MR examination within 15 seconds. J Magn Reson Imaging 2001;14:300–305.
23. Sheehan FT, Zajac FE, Drace JE. Using cine phase contrast magnetic resonance imaging to non-invasively study in vivo knee dynamics. J Biomech 1998;31:21–26.
24. D'Entremont AG, Nordmeyer-Massner JA, Bos C, et al. Do dynamic-based MR knee kinematics methods produce the same results as static methods? Magn Reson Med. 2012 [Epub ahead of print].
25. Busse H, Thomas M, Seiwerts M, et al. In vivo glenohumeral analysis using 3D MRI models and a flexible software tool: feasibility and precision. J Magn Reson Imaging 2008;27:162–170.
26. Poppen NK, Walker PS. Normal and abnormal motion of the shoulder. J Bone Joint Surg Am 1976;58:195–201.
27. Gilles B, Perrin R, Magnenat-Thalmann N, et al. Bone motion analysis from dynamic MRI: acquisition and tracking. Acad Radiol 2005;12:1285–1292.